ENDOCRINE SOCIETY

OXFORD

Gene Misexpression in a *Smoc2*+ve/*Sox2*-Low Population in Juvenile *Prop1*-Mutant Pituitary Gland

Bailey E. Masser,[1] Michelle L. Brinkmeier,[1] Yuxuan Lin,[2] Qin Liu,[2] Aya Miyazaki,[2] Jannatun Nayeem,[2] and Leonard Y. M. Cheung[2]

[1]Department of Human Genetics, University of Michigan Medical School, University of Michigan, Ann Arbor, MI 48105, USA
[2]Department of Physiology & Biophysics, Renaissance School of Medicine, Stony Brook University, Stony Brook, NY 11794, USA

Correspondence: Leonard Y. M. Cheung, PhD, Department of Physiology & Biophysics, Renaissance School of Medicine, Stony Brook University, 100 Nicolls Rd, Stony Brook, NY 11794, USA. Email: leonard.cheung@stonybrook.edu.

Abstract
Mutations in the pituitary-specific transcription factor Prophet of Pit-1 (*PROP1*) are the most common genetic etiology of combined pituitary hormone deficiency (CPHD). CPHD is associated with short stature, attributable to growth hormone deficiency and/or thyroid-stimulating hormone deficiency, as well as hypothyroidism and infertility. Pathogenic lesions impair pituitary development and differentiation of endocrine cells. We performed single-cell RNA sequencing of pituitary cells from a wild-type and a *Prop1*-mutant P4 female mouse to elucidate population-specific differential gene expression. We observed a *Smoc2*+ve population that expressed low *Sox2*, which trajectory analyses suggest are a transitional cell state as stem cells differentiate into endocrine cells. We also detected ectopic expression of *Sox21* in these cells in the *Prop1^{df/df}* mutant. *Prop1*-mutant mice are known to overexpress *Pou3f4*, which we now show to be also enriched in this *Smoc2*+ve population. We sought to elucidate the role of *Pou3f4* during pituitary development and to determine the contributions of *Pou3f4* upregulation to pituitary disease by utilizing double-mutant mice lacking both *Prop1* and *Pou3f4*. However, our data showed that *Pou3f4* is not required for normal pituitary development and function. Double mutants further demonstrated that the upregulation of *Pou3f4* was not causative for the overexpression of *Sox21*. These data indicate loss of *Pou3f4* is not a potential cause of CPHD, and further studies may investigate the functional consequence of upregulation of *Pou3f4* and *Sox21*, if any, in the novel *Smoc2*+ve cell population.

Key Words: pituitary, Prop1, Pou3f4, scRNA seq

Abbreviations: ACTH, adrenocorticotropic hormone; CPHD, combined pituitary hormone deficiency; Dko, double-knockout; EMT, epithelial-to-mesenchymal transition; PRL, prolactin; GH, growth hormone; qPCR, quantitative polymerase chain reaction; scRNAseq, single-cell RNA sequencing; TSH, thyrotropin (thyroid-stimulating hormone); UMAP, uniform manifold approximation and projection; WT, wild-type.

The pituitary gland is a neuroendocrine regulator which secretes hormones that are critical for the regulation of many physiological processes. Situated at the base of the brain, directly below the hypothalamus, the pituitary is divided into 3 lobes with dual developmental origins. Pituitary organogenesis begins around week 4 of human development and embryonic day 8 (E8) in mice, during which the neuroectoderm on the floor of the diencephalon gives rise to the posterior lobe [1, 2]. The anterior pituitary houses 5 distinct cell types, including somatotropes, lactotropes, gonadotropes, thyrotropes, and corticotropes. Upon receiving specific hypothalamic signals, these cell types are responsible for releasing the peptide hormones growth hormone (GH), prolactin (PRL), luteinizing hormone (LH) and follicle-stimulating hormone (FSH), thyroid-stimulating hormone (TSH), and adrenocorticotropic hormone (ACTH), respectively. These hormones, in turn, signal peripheral organs to regulate processes such as growth, lactation, fertility, metabolism, and stress response. With vital functions throughout the body, deficiencies in pituitary hormones can be fatal if left untreated.

Combined pituitary hormone deficiency (CPHD) is characterized by a shortage of GH and at least one other pituitary hormone. Due to these deficiencies, children with CPHD present with short stature, hypothyroidism, hypoglycemia, and hypogonadism [3]. CPHD is relatively common, affecting an estimated 1 in 8000 newborns worldwide [4]. To date, more than 60 genes are known to be implicated in the pathogenesis of CPHD, with mutations often impairing embryonic pituitary development and differentiation of endocrine cells in humans and mice [5-7]. Loss-of-function mutations in the pituitary-specific transcription factor Prophet of Pit-1 (*Prop1*) are the most common genetic etiology, accounting for 12% to 55% of cases in different cohorts [4, 5]. PROP1 is required to activate another pituitary transcription factor, POU Domain Class 1, Homeobox 1 (POU1F1, also known as *Pit-1*), to drive the differentiation of progenitor cells into cells that produce TSH, GH, or PRL, and mutations in POU1F1 also cause CPHD in humans and mice [8]. PROP1 alternatively induces other genes, such as Zinc Finger E-box Binding Homeobox 2 (*Zeb2*) and Notch Receptor 2 (*Notch2*) to regulate the epithelial-to-mesenchymal transition (EMT)-like process of differentiating stem cells, independent of POU1F1 [9], suggesting PROP1 has additional downstream targets that are necessary for normal pituitary

development and function. Due to defects in these regulatory pathways, patients with *PROP1* mutations typically present with progressive hormone deficiencies involving TSH, GH, PRL, and gonadotropins, and sometimes evolving to a life-threatening loss of ACTH. However, there is phenotypic heterogeneity among patients, with variable age of onset, effect on pituitary size, and the number and type of hormone deficiencies [10].

Prop1-null mice exhibit congenital TSH, GH, and PRL deficiencies, making them a compelling model organism to study disease pathophysiology and develop potential human therapies. *Prop1*-mutant mice show elevated expression of several genes, including *Hesx1* and *Pou3f4* [11, 12], indicating that PROP1 functions as an important transcriptional repressor. In this study, we performed single-cell RNA sequencing (scRNAseq) of pituitary cells from individual P4 female wild-type and *Prop1^{df/df}* mutant mice to gain cell-type–specific resolution of differential gene expression in the absence of *Prop1* function. We observed gene misexpression, including upregulated *Pou3f4* as well as ectopic *Sox21* expression, in a novel subset of *Sox2*-lowly expressing cells in the juvenile pituitary gland. RNA velocity trajectory analysis suggests that this population, marked by expression of *Smoc2*, comprises intermediary cells as stem cells differentiate into endocrine cells. We generated *Pou3f4*; *Prop1* double-mutant mice but did not observe reversal of *Sox21* ectopic expression or other changes from *Prop1*-mutant phenotypes. Therefore, we have identified that *Prop1* is required to maintain proper gene expression in a novel juvenile *Smoc2*+ve/*Sox2*-low cell population.

Methods

Mouse Strains

The use of mice at the University of Michigan was approved by the University of Michigan's Animal Care and Use Program and the Institutional Animal Care & Use Committee (IACUC). Husbandry was provided by the Unit for Laboratory Animal Medicine (ULAM). Mice were housed under standard light/dark conditions and provided food ad libitum. All mouse strains used in this study have been previously published. The *Prop^{tm1Sac}* allele is functionally null and homozygous mice are mutants with the same phenotypes as the *Prop1^{df/df}* spontaneous mutants. The *Prop^{tm1Sac}* allele is more simply referred to as *Prop^−*. *Sox21^{−/−}* knockout mice were previously generated [13, 14]. *Pou3f4*del-J(C3HeB/FeJ-*Pou3f4*^{del−J}/J), JAX Stock No.: 004406 (RRID: IMSR_JAX:004406) [15]. *Prop1^{df}* JAX Stock No.: 001618 [16]. *Prop1^−* MGI: 3521736 [10]. *Pou1f1^{dw}* JAX Stock No.: 000772 [12].

Genotyping

Genotyping for the *Prop1^{df}* allele was performed as previously described using PCR and *HinfI* restriction digest [17]. Genotyping for the *Pou1f1^{dw}* allele was performed by PCR and *AvaII* digest as previously described [12]. Genotyping for *Pou3f4* and the sex chromosomes were performed in the same reaction, using primers for the *Pou3f4* CDS and primers that amplify different products from the homologous genes, *Uba1* on the X chromosome, and *Uba1y* on the Y chromosome. The *Pou3f4* and *Uba1y* primers were designed using the National Center for Biotechnology Information (NCBI)

Primer-Basic Local Alignment Search Tool (BLAST). *Prop1^{tm1Sac}* genotyping was performed in 2 separate PCRs, independently from the *Pou3f4* and sex genotyping as previously described [10]. PCR products were run on a 1.5% agarose gel and visualized using SYBR Safe. *Prop1^{+/df}* F, 5′—GAGCTGGGGAGACCTAAGCTTTGCC—3′. *Prop1^{+/df}* R 5′—GCCCAGATGTCAGGATACTG—3′. *Pou1f1^{+/dw}* F 5′—GCTGCTAAGGATGCTCTGG—3′. *Pou1f1^{+/dw}* R 5′—CCTTGGAAATAGAGAACAGGC –3′. *Prop1* (F) 5′—GTGAGAAAACAGGTATCTAGCT—3′. *Prop1 ^{tm1Sac}* (R) 5′—CTTACTTCCACCTACTCACTTCC—3′. *Prop1* WT (R) 5′—TTCGTTTGCTTTTCCTGTG—3′. *Pou3f4* CDS (F) 5′—CCCCGCACCATAGATGTCAA—3′. *Pou3f4* CDS (R) 5′—CCCCTGTGAAAGAAAAGAGC—3′. *Uba1y* (F) 5′—TGGATGGTGTGGCCAATG—3′. *Uba1y* (R) 5′—CACCTGCACGTTGCCCTT—3′.

Quantitative PCR

mRNA from mouse pituitaries was prepared using the QIAGEN RNeasy Mini Kit (Catalog No.: 74104). cDNA was synthesized using the Invitrogen SuperScript First-Strand Synthesis System for RT-PCR (Catalog No.:1190418). All reactions were prepared as suggested by the manufacturer. The quantitative polymerase chain reactions (qPCRs) were performed on an Applied Biosystems 7500 Real-Time PCR Instrument using TaqMan Universal PCR Master Mix (Catalog No.: 4304437). Hypoxanthine Guanine Phosphoribosyltransferase (*Hprt*) expression was used as the housekeeping control. Comparative mRNA expression was calculated using the $2^{−ΔΔCt}$ method and data were plotted in GraphPad Prism 9. Statistical tests were performed in R Studio or Prism and differences between groups were analyzed by unpaired *t* test. TaqMan Probe mouse assays (Catalog No.: 4331182): *Lhb* mm00656868_g1; *Nr5a1* mm00446826_m1; *Pou1f1* mm00476852_m1, *Smoc2* mm00491553_m1; *Sox21* mm00844350_s1; *Sox2* mm03053810_s1; *Hprt* mm03024075_m1.

Single-Cell RNA Library Preparation

ScRNAseq RNA libraries were prepared from one P4 female *Prop1^{+/+}* pituitary gland and one P4 female *Prop1^{df/df}* pituitary gland from the same litter. Single-cell RNA libraries were prepared by the University of Michigan's Advanced Genomics Core on the 10× Genomics Chromium 3′ Gene Expression v3 platform following the manufacturer's instructions and sequenced on the NovaSeq6000 platform with an S4 chip.

Single-Cell Sequencing Computation Analyses

Samples were analyzed similarly to our previous studies [18]. Samples were demultiplexed and fastq files aligned using Cellranger Single Cell Software Suite 3.1.0. Sequence reads were aligned to a modified mm10 containing extended annotation for the Prop1 3′ untranslated region [19]. Binary sequence alignment maps were converted into loom files using velocyto.py [20] and imported into R for primary analyses using Seurat 3.1.2 and 5.1.0 [21, 22]. Core Seurat functions were used to import loom files, integrate samples, generate uniform manifold approximation and projection (UMAP), calculate clusters, and calculate differential gene expression. Expression plots used Nebulosa 1.12.1 [23]. Plots and images

generated in R or Excel were compiled in Adobe Photoshop 2024. Sequencing data are available on National Center for Biotechnology Information Gene Expression Omnibus accession number GSE273683, and web-based expression visualization are viewable on the Broad Single Cell Portal at SCP2695.

Immunohistochemistry

Mouse postnatal heads were collected, paraffinized and sectioned on a coronal plane at 5 μm. Immunostaining of paraffin sections was performed using the Biotium Tyramide Amplification Kit with horseradish peroxidase-streptavidin and CF AlexaFluor 594 tyramide (TSA) (Biotium Catalog No.: 33009). Following dewaxing, epitopes were unmasked using citric acid. Endogenous peroxidases were quenched in 50% methanol and 3% hydrogen peroxide. Nonspecific reactions were blocked with a TSA block containing 10% donkey serum and 5% bovine serum albumin (BSA). Sections were treated with goat anti-human SOX21 antibody (R&D Systems AF3538 [RRID: AB_2195947, https://scicrunch.org/resolver/RRID:AB_2195947], 1:100) overnight at 4 °C followed by biotinylated donkey anti-goat secondary antibody (Invitrogen D-20698 [RRID: AB_2536519, https://scicrunch.org/resolver/RRID:AB_2536519], 1:500) for 1 hour at room temperature. The tertiary reaction with horseradish peroxidase-streptavidin was applied for 1 hour at room temperature before treating with the TSA-CF594 at 1:500 for 10 minutes. Slides were mounted using Invitrogen Molecular Probes ProLong Diamond Antifade Mountant with DAPI (Catalog No.: P36971, Lot No.: 2384717). Imaging was conducted using a Leica Leitz DM RP upright microscope and images were compiled and adjusted for clarity in Adobe Photoshop 2024.

RNAscope

RNAscope mRNA visualization was performed using the RNAscope 2.5 HD Duplex Detection Kit (Advanced Cell Diagnostics 322500) with the *Smoc2* probe in red (C1) (318541) and the *Slc16a2* probe in blue (C2) (545291-C2) following manufacturer's protocol. Target retrieval was performed by boiling in retrieval buffer for 7 minutes, and protease digestion for 20 minutes.

Results

Single-Cell RNA Sequencing of Prop1-Mutant Pituitary Cells

We performed scRNAseq on pituitary glands from one P4 *Prop1*$^{+/+}$ female and one P4 *Prop1*$^{df/df}$ female on the 10× Genomics Chromium 3′ Gene Expression v3 platform targeting 10 000 cells from each sample. After filtering for cells with > 500 genes/cell, between 2000 and 20 000 transcripts per cell, and < 5% mitochondrial transcripts, we recovered 7893 cells from the wild-type and 5830 cells from the mutant (Fig. 1A). Computational clustering with Seurat detected 20 clusters (Fig. 1B), which were assigned identities based on expression of cell-type signature genes (Supplementary Fig. S1 [24]). All expected cell types were detected. Lactotropes were not detected, which was expected due to low number of lactotropes and low prolactin expression in juvenile mice. Two clusters were made up almost solely of cells in G2M/S phase, representing proliferating *Sox2* stem cells and

proliferating *Pou1f1*+ve cells (Fig. 1C). The composition of the *Prop1*$^{df/df}$ sample had fewer *Pou1f1* lineage cells (somatotropes, thyrotropes, proliferating *Pou1f1* cells) as expected and proportionally more gonadotropes and corticotropes (Fig. 1D). A small number of oligodendrocyte precursors expressing *Olig1* and *Olig2* were detected, with more in the *Prop1*$^{df/df}$ sample. This was likely due to accidental inclusion of neural tissue during the dissection. Accordingly, *Pou1f1* expression is essentially absent from *Prop1*$^{df/df}$ cells (Fig. 1E). *Prop1* transcripts are detected in the *Prop1*$^{df/df}$ mutant as the *df* mutation causes a missense mutation that inactivates the homeobox. The majority of *Sox2*-expressing cells was divided into 3 clusters: proliferating *Sox2* cells (Fig. 1F), and parenchymal and cleft *Sox2* stem cells based on recent description [25] of higher expression of *Aqp3* in the parenchymal stem cells (Fig. 1G) and *Ednrb* in cleft stem cells (Fig. 1H). Expression of thyroid hormone transporter *Slc16a2* (*Mct8*) appears higher in the cleft stem cells (Fig. 1I).

Detection of a Transient Juvenile *Sox2*-Low Subpopulation in Mouse Pituitary

Several computational clusters expressed *Sox2* (Fig. 1F, Fig. 2A). We examined one cell cluster that expressed lower *Sox2* than the major *Sox2* stem cell clusters (Fig. 2A arrow, cluster 6). This cluster has unique gene expression, the most significant of which was SPARC-related modular calcium binding protein 2 (*Smoc2*) (Fig. 2B and C). This population was absent from previous scRNAseq data from wild-type P49 male mouse pituitary cells [19] and present in other juvenile samples from P4 and P7 mice [18, 26]. RNA velocity trajectory analysis with Velocyto setting the cleft stem cells as the root suggested that the *Smoc2* population represented an intermediary cell state as stem cells differentiated into endocrine cells (Fig. 2D). Quantitative PCR for *Smoc2* from wild-type pituitaries from embryos, newborn/juvenile, and 2- and 3-week-old mice showed that *Smoc2* expression is highest in the first week of life (Fig. 2E). RNAscope for *Smoc2* and *Slc16a2* transcripts in P7 female control pituitary glands showed diffuse location of *Smoc2* expression throughout the gland, while *Slc16a2* expression was enriched along the cleft (Fig. 2F).

Ectopic Gene Expression in the *Smoc2*+ve Population in *Prop1*$^{df/df}$ Mutants

We examined differential gene expression within the *Smoc2*+ve population between the *Prop1*$^{df/df}$ and the wild-type to explore how the loss of *Prop1* activity impacts this population. We detected expression of *Sox21* in the *Smoc2*+ve population, specifically from *Prop1*-mutant cells in the *Smoc2*+ve cluster (Fig. 3A and 3B). *Sox21* is not normally detected in the pituitary gland [13], so its expression is ectopically activated without *Prop1*. We validate by qPCR that *Sox21* is highly upregulated in *Prop1*$^{df/df}$ pituitary glands at P7 (Fig. 3C); the very large fold change is due to comparison to almost zero expression in the controls. We observed no change in *Sox21* expression in *Pou1f1*$^{dw/dw}$ mutant mice, another mouse model of CPHD which lacks GH, PRL and TSH as in the *Prop1*$^{df/df}$ but have normal ACTH and gonadotropins, showing that the ectopic expression was a specific effect of the loss of *Prop1* action. Finally, we detected SOX21 protein in the *Prop1*$^{df/df}$ pituitary gland at P3 and P7 (Fig. 3D).
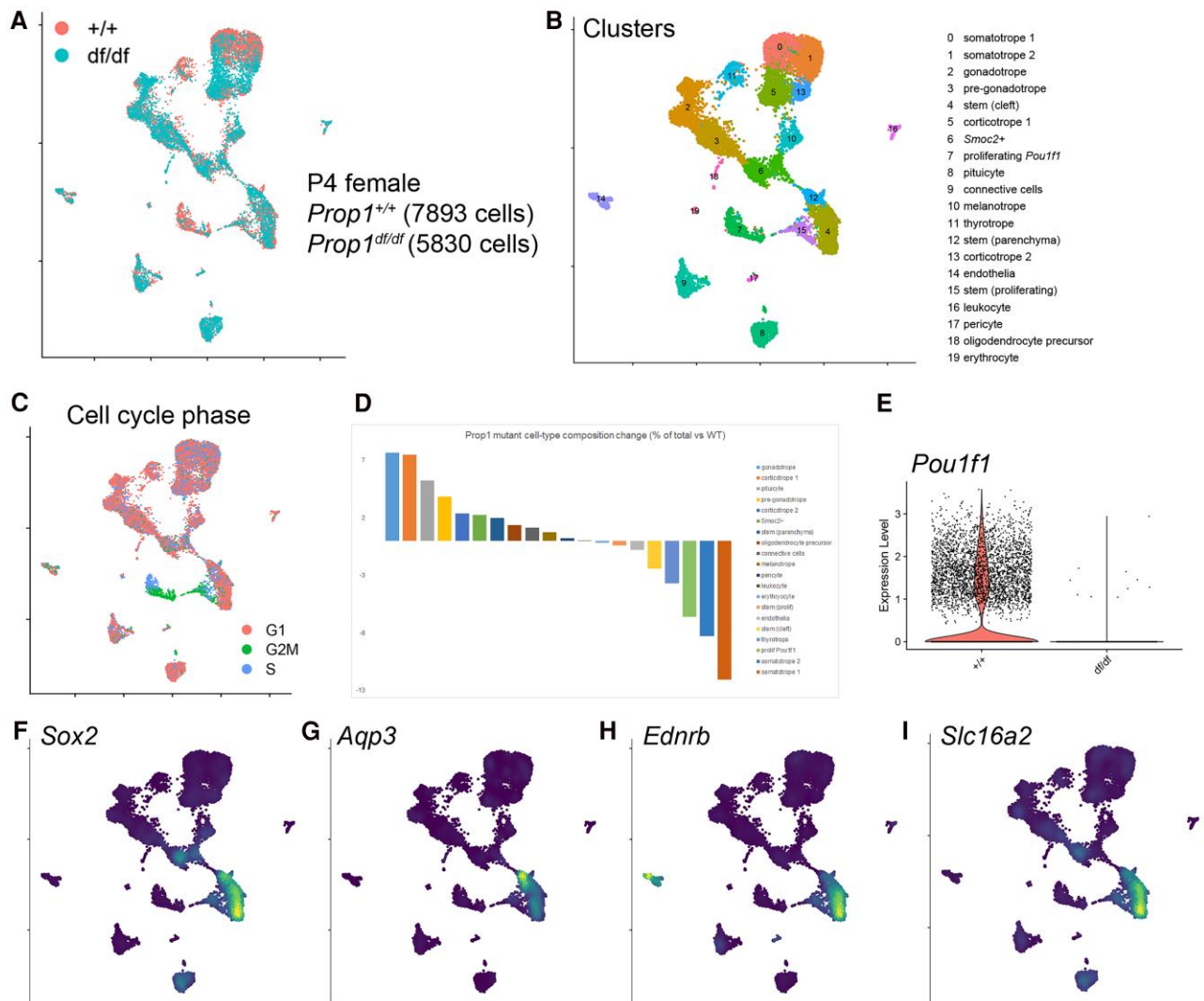
Figure 1. Single-cell sequencing of wild-type and *Prop1*-mutant P4 female pituitary cells. (A) UMAP of integrated wild-type and mutant cells. The mutant lacks cells from certain cell populations (detailed below). (B) Computational clustering and assignment of likely identity (see Supplementary Fig. S1 [24]). (C) Difference in cell-type proportions in *Prop1*-mutant mice. *Prop1*-dependent cell types such as somatotropes, thyrotropes, and proliferating *Pou1f1*-cells are depleted in the *Prop1*-mutant as expected. As a result, gonadotropes and corticotropes are proportionally enriched. (D) Cell cycle phase scoring, identifying proliferating stem cells and *Pou1f1*+ve cells. (E) Absence of *Pou1f1* expression in the *Prop1*-mutant sample. (F-I) Expression of *Sox2* and other markers that differentiate the cleft and parenchymal stem cells.

Known Upregulation of *Pou3f4* in *Prop1^{df/df}* Mutants Occurs in the *Smoc2*+ve Population, Although Double Deletion of *Pou3f4* and *Prop1* Does Not Reverse *Prop1*-Mutant Phenotypes

We also observed expression of other transcription factors in the *Smoc2*+ve population, including *Lef1* and *Pou3f4* (*Brn4*) (Fig. 4A). Upregulation of *Pou3f4* in *Prop1^{df/df}* mutant mice has been previously reported [11]. With cell-type resolution from scRNAseq we determined that the upregulation of *Pou3f4* occurs primarily in the *Smoc2*+ve population (Fig. 4B). *Pou3f4* is X-linked in mice and hemizygous males and homozygous females develop deafness, but pituitary glands in these mice have not been described. Histology of *Pou3f4* mutant was normal at P1 (Fig. 3C, males shown, females also normal). While deletion of *Pou3f4* did not appear to have any influence on gross pituitary morphology or anterior lobe development, we wanted to determine if there were transcriptional defects in markers of stem cell maintenance

or differentiation. We applied qPCR to samples from P1 wild-type (WT) and *Pou3f4*-mutant pituitaries to detect changes in expression of the stem cell marker *Sox2*, and the endocrine progenitor marker *Pou1f1* (Fig. 4D). There were no significant changes in *Sox2* or *Pou1f1* expression between hemizygous-WT controls and *Pou3f4*-mutant males, *Pou3f4*-mutant females, or *Pou3f4* mutants of both sexes. This suggested that loss of *Pou3f4* does not influence *Sox2* stem cell maintenance and *Pou1f1* endocrine progenitor differentiation.

To determine if *Prop1*-mutant phenotypes, including ectopic expression of *Sox21* in *Smoc2*+ve cells, are attributable to *Pou3f4* upregulation, we generated *Pou3f4^{−/−}*; *Prop1^{−/−}* double-knockout (dKO) mice. We obtained slightly fewer *Prop1* mutants and dKOs than expected (chi-square statistic value, *P* value = .0225) (Supplementary Fig. S2 [27]). dKO mice were dwarfed akin to *Prop1*-mutant mice postnatally, and we did not observe rescue of pituitary dysmorphology or hypoplasia of *Prop1*-mutant mice in embryonic and
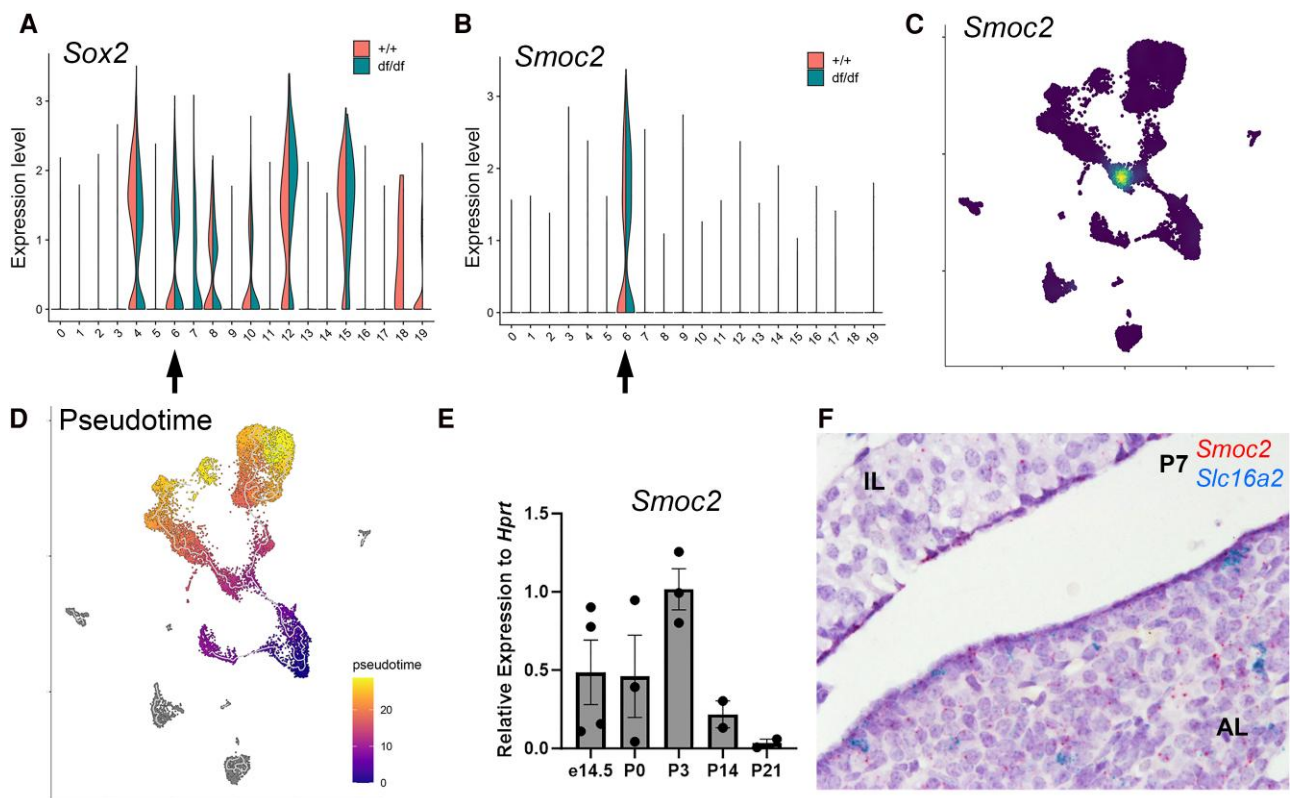
Figure 2. Detection of a transient juvenile *Sox2*-low cell state in mouse pituitary. (A) Violin plot of *Sox2* expression across calculated clusters. Cluster 6 cells express *Sox2*, albeit lower than some other clusters. (B, C) Cluster 6 cells uniquely express *Smoc2*. (D) RNA velocity trajectory analysis setting the cleft *Sox2*+ve stem cells as the root suggests stem cells pass through the *Smoc2*+ve cluster 6 as they differentiate into endocrine cells. (E) qPCR for *Smoc2* from control pituitary glands at young ages show highest expression at P3. (F) RNAscope detection of diffuse *Smoc2* transcripts and *Slc16a2* in cleft cells in female P7 mouse pituitary.

newborn dKOs (Supplementary Fig. S2C and 2D [27]). We sought to address whether deletion of *Pou3f4* would reduce the overexpression of *Sox21* observed in *Prop1*-mutant mice. We applied qPCR to samples from P21 WT, *Pou3f4*-single-mutant, *Prop1*-single-mutant, and dKO pituitaries to compare the levels of *Sox21* mRNA expression (Fig. 4E). However, when comparing the dKO mice to the controls, the elevation of *Sox21* expression remains significant (P value = .02875), and there is not a significant difference in the level of expression between the *Prop1*-single-mutant and dKO mice (P value = .4). Considering levels of *Sox21* mRNA expression were comparable between *Prop1*-mutant and dKO pituitaries, the upregulation of *Pou3f4* is not required for the overexpression of *Sox21* in *Prop1*-mutant mice. Upregulation of *Smoc2* and *Nr5a1* in the *Prop1*-mutants were similarly unaffected by the additional loss of *Pou3f4*. As a result, it is not clear whether the upregulation of *Pou3f4* in the *Prop1*-mutant pituitary has a functional effect.

Discussion

Mutations in *Prop1* are the most common genetic etiology of CPHD [4]. *Prop1* functions to regulate the EMT-like process of differentiating stem cells and activate *Pou1f1* to drive differentiation of progenitors into hormone-producing cells [8, 9]. Consequently, defects in *Prop1* impair the migration of stem cells and the differentiation of endocrine cells. This leads to hypoplasia of the anterior lobe, misfolding, and endocrine defects, which are hallmarks of *Prop1* mutations. Our

scRNAseq of wild-type and *Prop1*-mutant cells provided the first cell-type–specific differential gene expression analyses occurring in *Prop1*-mutant pituitary gland. We observed expected gene expression and cell population changes such as reduced *Pou1f1*-lineage endocrine cell numbers, as well as differentiate between cleft and parenchymal *Sox2*-expressing pituitary stem cells based on higher expression of markers such as *Aqp3* (parenchyma) and *Ednrb* (cleft) [25]. We also observed expression of the thyroid hormone transporter *Slc16a2* (also called *Mct8*) with higher expression in cleft stem cells, which was also observed by RNAscope (Fig. 1). *SLC16A2* genetic mutations in humans cause Allan Herndon Dudley Syndrome characterized by neurodevelopmental delay, but pituitary phenotypes in these patients are unclear [28].

We observed a cell population not corresponding to any expected cell-type in both the wild-type and *Prop1*-mutant samples. This population expressed *Sox2* albeit at a lower level than the major clusters representing parenchymal, cleft, and proliferating *Sox2*+ve stem cells (Fig. 2). UMAP and RNA velocity trajectory analyses suggest that this population is an intermediary or transitional cell state as stem cells differentiate into endocrine cells (Fig. 2D). The most enriched marker of this population was *Smoc2*, an extracellular calcium binding glycoprotein, which is implicated in a variety of physiological and pathological processes. It is an intestinal stem cell marker associated with better survival in colorectal cancers [29], promotes EMT in renal cell carcinoma [30], regulates bone formation and healing [31, 32], and human mutations in
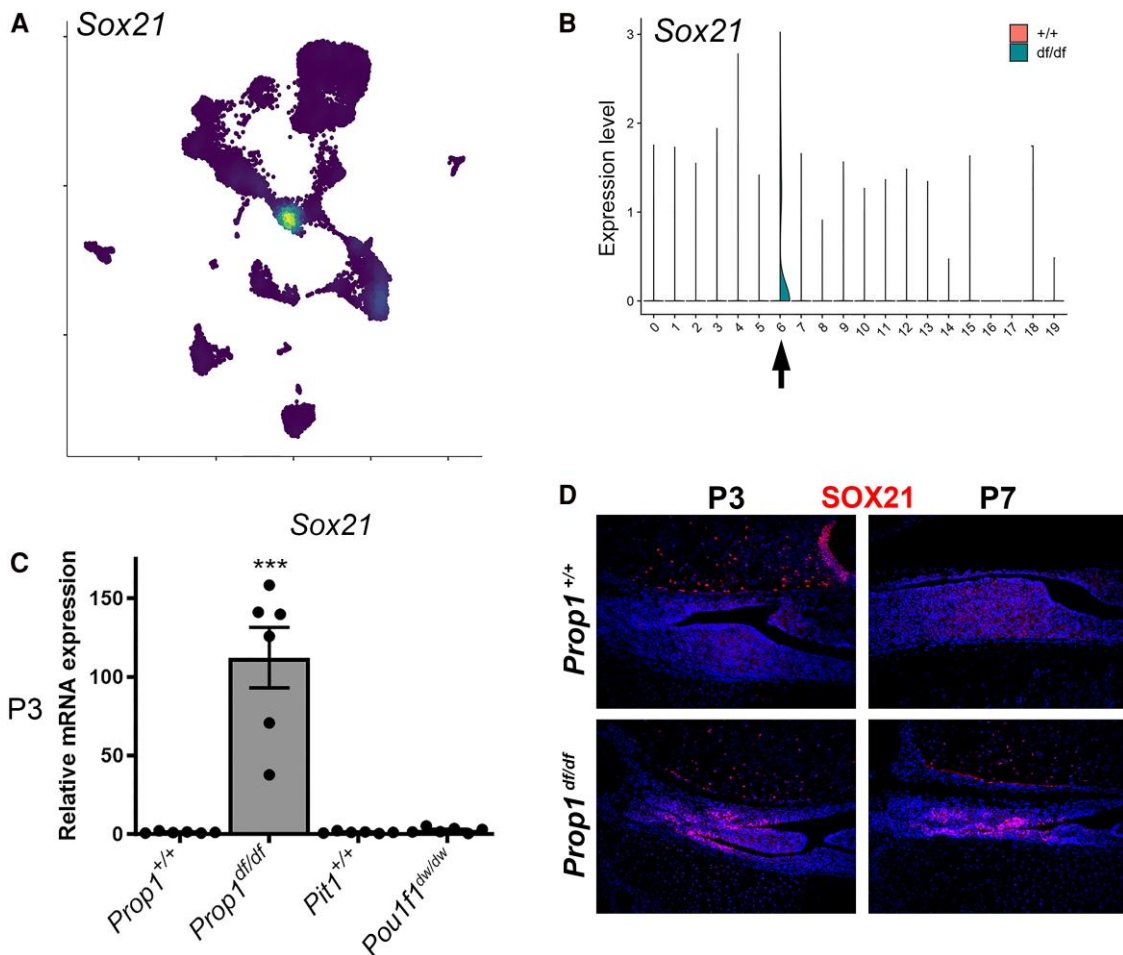
Figure 3. Ectopic expression of *Sox21* in the *Smoc2*-expressing population in *Prop1^{df/df}* mice. (A-B) Sox21 is upregulated in *Prop1*-mutants in cluster 6, the *Sox2/Smoc2* population. (C) *Sox21* upregulation occurs in *Prop1^{df/df}* mutants but not *Pou1f1^{dw/dw}* mutants, another model of pituitary hormone deficiency. (D) SOX21 ectopic expression in *Prop1^{df/df}* pituitary glands in P3 and P7 mice.

SMOC2 can cause dental developmental defects [33] and growth plate defects [34]. A previous study with functionally null homozygous *Smoc2-GFP-ires-CreERT2* knock-in mice had no reported gross phenotypes [35], although the International Mouse Phenotyping Consortium reports bone defects and weight and length reductions in *Smoc2^{tm1.1}* homozygous null mice, suggesting further studies may be needed to identify whether these growth reductions are due to bone and/ or pituitary defects. *Smoc2*-expressing cells are detected in our previous P7 scRNAseq dataset ([18]Single Cell Portal SCP2110) but not in our P49 postnatal dataset ([19]SCP2058), corroborating qPCR data here that showed *Smoc2* expression peaking in the first week of life in mice (Fig. 2E).

Pou3f4 is highly expressed during pituitary organogenesis from e10.5 until e14.5 in Rathke's pouch and the developing anterior lobe [11]. The endogenous function of *Pou3f4* in the pituitary and the contributions of its upregulation to *Prop1*-mutant phenotypes have not been described. However, we have shown that *Pou3f4* is not necessary for normal pituitary morphology, maintenance of *Sox2*-expressing stem cells, or differentiation of *Pou1f1* endocrine progenitors. Consistent with these results, *Pou3f4*-mutant mice did not exhibit reduced growth, craniofacial defects, or infertility, which are indicative of hormone deficiencies.

Genetic defects in *Pou3f4* cause nonsyndromic X-linked deafness 2 (DFNX2) (also known as conductive deafness with stapes fixation 3 [DFN3]) in humans and mice, which is the most common form of X-linked deafness [36, 37]. At the same time, *Sox21*-mutant mice also manifested hearing defects, exhibiting a higher decibel threshold for eliciting an auditory brainstem response [38], although *SOX21* variants have not yet been associated with a human disease. Both the inner ear and pituitary gland derive from cranial placodes [39] (otic and adenohypophyseal placodes respectively) and express some shared transcription factors during development, for example *Six1* and *Eya1* [40-42], although loss of *Six1* or *Eya1* both affect otic placode development, while loss of both is required to cause pituitary defects [40]. We speculate whether the loss of *Prop1*, a pituitary-specific transcription factor, may lead to de-repression of genes normally expressed in other placodes, although we note that there does not appear to be transdifferentiation of pituitary cells into otic cells and we do not observe expression of otic markers such as *Pax8*.

Gene overexpression can impair pituitary development, for example transgenic mice with constitutively expressed HESX1 have impaired thyrotrope and gonadotrope differentiation [43]. We therefore sought to determine if any
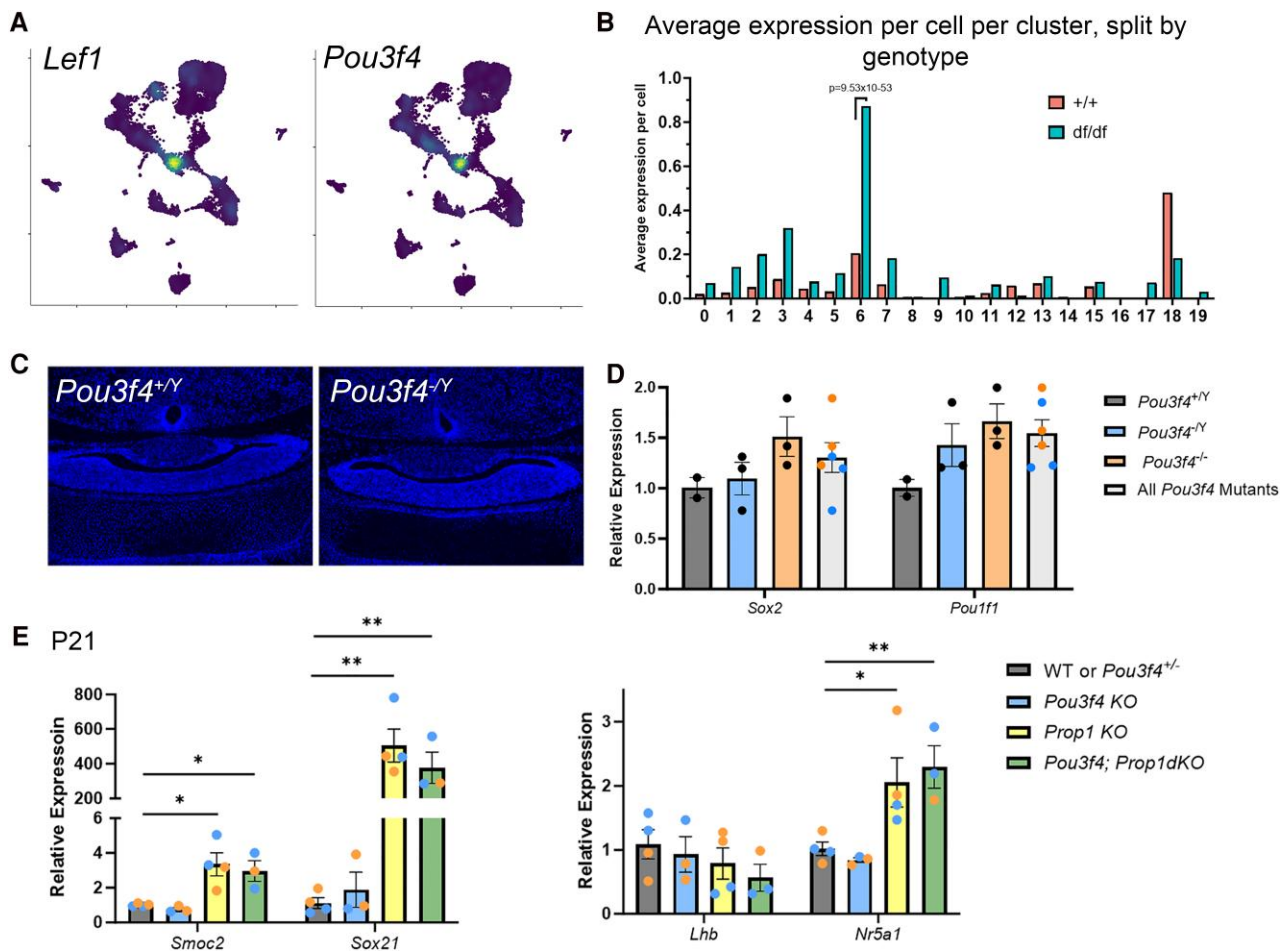
Figure 4. *Pou3f4* overexpression in *Prop1*-mutants occurs in *Smoc2/Sox2* cells but does not appear to drive *Sox21* overexpression. (A) Transcription factors such as *Lef1* and *Pou3f4* are also expressed specifically in the *Smoc2*+ve population. (B) Average *Pou3f4* expression per cell per cluster, split by genotype, is significantly increased in the *Smoc2*-expressing cluster 6 in *Prop1*-mutant cells. (C) P1 *Pou3f4*-mutant mice have normal pituitary morphology and (D) *Sox2* and *Pou1f1* expression are normal. (E) Double deletion of *Prop1* and *Pou3f4* does not reverse *Prop1*-mutant phenotypes such as *Sox21* ectopic expression or hypoplasia and dysmorphology (Supplementary Fig. S2 [27]). For D-E, blue points represent male samples and orange points represent female samples.

Prop1-mutant phenotypes are attributable to *Pou3f4* upregulation. However, we found that *Pou3f4* upregulation is not necessary for the gross dysmorphology, hypoplastic anterior lobe, or upregulation of *Sox21* in *Prop1*-mutant mice. This suggested that *Pou3f4* may not be a critical transcriptional regulator in the *Prop1*-mutant pituitary. The lack of rescue is not likely to be related to the age of tissues collected, as we observe generally no difference between *Prop1*-mutant and dKOs at e16.5, P3, or P21 by a combination of histology and qPCR.

An alternative model to the one proposed in this study is that *Prop1* represses *Sox21*, which regulates *Pou3f4*. In this case, the loss of *Prop1* would cause the upregulation of *Sox21*, which would lead to the overexpression of *Pou3f4*. We were only able to collect pituitary tissue from one *Sox21*; *Prop1* double-mutant mouse, but growth phenotypes of the *Prop1* and *Sox21* mutations were additive. Double mutants were in poor health postnatally and the experiment was discontinued (Supplementary Fig. S3 [44]). Pituitary dysmorphology and hypoplasia was not rescued in one postnatal 3-week-old mutant, suggesting that *Sox21* overexpression does not drive pituitary dysmorphology or hypoplasia in *Prop1*-mutant mice, although it does leave the possibility that ectopic expression of *Sox21* is transcriptionally upstream of *Pou3f4* upregulation in *Prop1*-mutants. Conversely, *Prop1* could be independently repressing *Pou3f4* and *Sox21*, leading to their simultaneous upregulation when *Prop1* is lost. We are not able to generate further *Prop1*; *Sox21* double-mutant mice for study.

Overall, this study has provided insights into population-specific gene expression changes in the *Prop1*-mutant pituitary gland including detection of a novel *Smoc2*+ve, *Sox2*-low population as well as how loss of *Prop1* causes gene misexpression in this population. While we found that *Pou3f4* overexpression did not cause overexpression of *Sox21* or dysmorphology in *Prop1*-mutant mice, future studies may explore the molecular mechanisms driving gene dysregulation in *Smoc2*+ve cells and its functional impact on Prop1 mutant phenotypes.

Acknowledgments

Funding

Disclosures

Authors have no conflicts of interest to disclose.

Data Availability

Original data generated and analyzed during this study are included in this published article or in the data repositories listed in "Methods" and "References."

References

1. Sheng HZ, Westphal H. Early steps in pituitary organogenesis. *Trends Genet*. 1999;15(6):236-240.
2. Kelberman D, Rizzoti K, Lovell-Badge R, Robinson IC, Dattani MT. Genetic regulation of pituitary gland development in human and mouse. *Endocr Rev*. 2009;30(7):790-829.
3. Dattani M, Preece M. Growth hormone deficiency and related disorders: insights into causation, diagnosis, and treatment. *Lancet*. 2004;363(9425):1977-1987.
4. De Rienzo F, Mellone S, Bellone S, *et al*. Frequency of genetic defects in combined pituitary hormone deficiency: a systematic review and analysis of a multicentre Italian cohort. *Clin Endocrinol (Oxf)*. 2015;83(6):849-860.
5. Fang Q, George AS, Brinkmeier ML, *et al*. Genetics of combined pituitary hormone deficiency: roadmap into the genome era. *Endocr Rev*. 2016;37(6):636-675.
6. Budny B, Zemojtel T, Kaluzna M, *et al*. SEMA3A and IGSF10 are novel contributors to combined pituitary hormone deficiency (CPHD). *Front Endocrinol (Lausanne)*. 2020;11:368.
7. Jee YH, Gangat M, Yeliosof O, *et al*. Evidence that the etiology of congenital hypopituitarism has a major genetic component but is infrequently monogenic. *Front Genet*. 2021;12:697549.
8. Li S, Crenshaw EB, Rawson EJ, Simmons DM, Swanson LW, Rosenfeld MG. Dwarf locus mutants lacking three pituitary cell types result from mutations in the POU-domain gene pit-1. *Nature*. 1990;347(6293):528-533.
9. Perez Millan MI, Brinkmeier ML, Mortensen AH, Camper SA. PROP1 triggers epithelial-mesenchymal transition-like process in pituitary stem cells. *Elife*. 2016;5:e14470.
10. Nasonkin IO, Ward RD, Raetzman LT, *et al*. Pituitary hypoplasia and respiratory distress syndrome in Prop1 knockout mice. *Hum Mol Genet*. 2004;13(22):2727-2735.
11. Sornson MW, Wu W, Dasen JS, *et al*. Pituitary lineage determination by the Prophet of Pit-1 homeodomain factor defective in Ames dwarfism. *Nature*. 1996;384(6607):327-333.
12. Gage PJ, Brinkmeier ML, Scarlett LM, Knapp LT, Camper SA, Mahon KA. The Ames dwarf gene, df, is required early in pituitary ontogeny for the extinction of Rpx transcription and initiation of lineage-specific cell proliferation. *Mol Endocrinol*. 1996;10(12):1570-1581.
13. Cheung LY, Okano H, Camper SA. Sox21 deletion in mice causes postnatal growth deficiency without physiological disruption of hypothalamic-pituitary endocrine axes. *Mol Cell Endocrinol*. 2017;439:213-223.
14. Kiso M, Tanaka S, Saba R, *et al*. The disruption of Sox21-mediated hair shaft cuticle differentiation causes cyclic alopecia in mice. *Proc Natl Acad Sci U S A*. 2009;106(23):9292-9297.
15. Gangon LH, Johnson KR. A spontaneous deletion of the Pou3f4 gene causing inner ear abnormalities. MGI Direct Data Submission. 2003. http://www.informatics.jax.org/downloads/Reference_texts/J83049.pdf
16. Andersen B, Pearse RV II, Jenne K, *et al*. The Ames dwarf gene is required for Pit-1 gene activation. *Dev Biol*. 1995;172(2):495-503.
17. Ward RD, Raetzman LT, Suh H, *et al*. Role of PROP1 in pituitary gland growth. *Mol Endocrinol*. 2005;19(3):698-710.
18. Cheung LYM, Menage L, Rizzoti K, *et al*. Novel candidate regulators and developmental trajectory of pituitary thyrotropes. *Endocrinology*. 2023;164(6):bqad076.
19. Cheung LYM, George AS, McGee SR, *et al*. Single-cell RNA sequencing reveals novel markers of male pituitary stem cells and hormone-producing cell types. *Endocrinology*. 2018;159(12):3910-3924.
20. La Manno G, Soldatov R, Zeisel A, *et al*. RNA velocity of single cells. *Nature*. 2018;560(7719):494-498.
21. Stuart T, Butler A, Hoffman P, *et al*. Comprehensive integration of single-cell data. *Cell*. 2019;177(7):1888-1902.e21.
22. Hao Y, Stuart T, Kowalski MH, *et al*. Dictionary learning for integrative, multimodal and scalable single-cell analysis. *Nat Biotechnol*. 2024;42(2):293-304.
23. Alquicira-Hernandez J, Powell JE. Nebulosa recovers single cell gene expression signals by kernel density estimation. *Bioinformatics*. 2021;37(16):2485-2487.
24. Masser BE, Brinkmeier ML, Lin Y, *et al*. Supplemental figure 1 for 'gene misexpression in a Smoc2+ve/Sox2-low population in juvenile Prop1-mutant pituitary gland'. *Figshare*. https://doi.org/10.6084/m9.figshare.26127232
25. Rizzoti K, Chakravarty P, Sheridan D, Lovell-Badge R. SOX9-positive pituitary stem cells differ according to their position in the gland and maintenance of their progeny depends on context. *Sci Adv*. 2023;9(40):eadf6911.
26. Cheung LYM, Camper SA. PROP1-dependent retinoic acid signaling regulates developmental pituitary morphogenesis and hormone expression. *Endocrinology*. 2020;161(2):bqaa002.
27. Masser BE, Brinkmeier ML, Lin Y, *et al*. Supplemental figure 2 for 'gene misexpression in a Smoc2+ve/Sox2-low population in juvenile Prop1-mutant pituitary gland'. *Figshare*. https://doi.org/10.6084/m9.figshare.26127238
28. Groeneweg S, van Geest FS, Abacı A, *et al*. Disease characteristics of MCT8 deficiency: an international, retrospective, multicentre cohort study. *Lancet Diabetes Endocrinol*. 2020;8(7):594-605.
29. Jang BG, Kim HS, Bae JM, Kim WH, Kim HU, Kang GH. SMOC2, an intestinal stem cell marker, is an independent prognostic marker associated with better survival in colorectal cancers. *Sci Rep*. 2020;10(1):14591.
30. Feng D, Gao P, Henley N, *et al*. SMOC2 promotes an epithelial-mesenchymal transition and a pro-metastatic phenotype in epithelial cells of renal cell carcinoma origin. *Cell Death Dis*. 2022;13(7):639.
31. Morkmued S, Clauss F, Schuhbaur B, *et al*. Deficiency of the SMOC2 matricellular protein impairs bone healing and produces age-dependent bone loss. *Sci Rep*. 2020;10(1):14817.
32. Takahata Y, Hagino H, Kimura A, *et al*. Smoc1 and Smoc2 regulate bone formation as downstream molecules of Runx2. *Commun Biol*. 2021;4(1):1199.
33. Bloch-Zupan A, Jamet X, Etard C, *et al*. Homozygosity mapping and candidate prioritization identify mutations, missed by whole-exome sequencing, in SMOC2, causing major dental developmental defects. *Am J Hum Genet*. 2011;89(6):773-781.
34. Long F, Shi H, Li P, *et al*. A SMOC2 variant inhibits BMP signaling by competitively binding to BMPR1B and causes growth plate defects. *Bone*. 2021;142:115686.
35. Munoz J, Stange DE, Schepers AG, *et al*. The Lgr5 intestinal stem cell signature: robust expression of proposed quiescent '+4' Cell markers. *EMBO J*. 2012;31(14):3079-3091.
36. Kok YJMd, van der Maarel SM, Bitner-Glindzicz M, *et al*. Association between X-linked mixed deafness and mutations

in the POU domain gene *POU3F4*. *Science*. 1995;267(5198): 685-688.

37. Choi BY, Kim DH, Chung T, *et al*. Destabilization and mislocalization of POU3F4 by C-terminal frameshift truncation and extension mutation. *Hum Mutat*. 2013;34(2):309-316.

38. Hosoya M, Fujioka M, Matsuda S, *et al*. Expression and function of Sox21 during mouse cochlea development. *Neurochem Res*. 2011;36(7):1261-1269.

39. Saint-Jeannet JP, Moody SA. Establishing the pre-placodal region and breaking it into placodes with distinct identities. *Dev Biol*. 2014;389(1):13-27.

40. Li X, Ohgi KA, Zhang J, *et al*. Eya protein phosphatase activity regulates Six1-Dach-Eya transcriptional effects in mammalian organogenesis. *Nature*. 2003;426(6964):247-254.

41. Nica G, Herzog W, Sonntag C, *et al*. Eya1 is required for lineage-specific differentiation, but not for cell survival in the zebrafish adenohypophysis. *Dev Biol*. 2006;292(1):189-204.

42. Xu PX, Adams J, Peters H, Brown MC, Heaney S, Maas R. Eya1-deficient mice lack ears and kidneys and show abnormal apoptosis of organ primordia. *Nat Genet*. 1999;23(1):113-117.

43. Carvalho LR, Brinkmeier ML, Castinetti F, Ellsworth BS, Camper SA. Corepressors TLE1 and TLE3 interact with HESX1 and PROP1. *Mol Endocrinol*. 2010;24(4):754-765.

44. Masser BE, Brinkmeier ML, Lin Y, *et al*. Supplemental figure 3 for 'gene misexpression in a Smoc2+ve/Sox2-low population in juvenile Prop1-mutant pituitary gland'. *Figshare*. https://doi.org/10.6084/m9.figshare.26127241